Protein phosphatase 4 controls circadian clock dynamics by modulating CLOCK/BMAL1 activity

Sabrina Klemz,[1,4] Thomas Wallach,[1,4] Sandra Korge,[1] Mechthild Rosing,[2] Roman Klemz,[1] Bert Maier,[1] Nicholas C. Fiorenza,[1] Irem Kaymak,[1] Anna K. Fritzsche,[1] Erik D. Herzog,[3] Ralf Stanewsky,[2] and Achim Kramer[1]

[1] Laboratory of Chronobiology, Charité-Universitätsmedizin Berlin, Corporate Member of Freie Universität Berlin and Humboldt-Universität zu Berlin,10117 Berlin, Germany; [2]Institute of Neuro and Behavioral Biology, Westfälische Wilhelms University, Münster 48149, Germany; [3]Department of Biology, Washington University in St. Louis, St. Louis, Missouri 63130, USA

In all organisms with circadian clocks, post-translational modifications of clock proteins control the dynamics of circadian rhythms, with phosphorylation playing a dominant role. All major clock proteins are highly phosphorylated, and many kinases have been described to be responsible. In contrast, it is largely unclear whether and to what extent their counterparts, the phosphatases, play an equally crucial role. To investigate this, we performed a systematic RNAi screen in human cells and identified protein phosphatase 4 (PPP4) with its regulatory subunit PPP4R2 as critical components of the circadian system in both mammals and *Drosophila*. Genetic depletion of PPP4 shortens the circadian period, whereas overexpression lengthens it. PPP4 inhibits CLOCK/BMAL1 transactivation activity by binding to BMAL1 and counteracting its phosphorylation. This leads to increased CLOCK/BMAL1 DNA occupancy and decreased transcriptional activity, which counteracts the "kamikaze" properties of CLOCK/BMAL1. Through this mechanism, PPP4 contributes to the critical delay of negative feedback by retarding PER/CRY/CK1δ-mediated inhibition of CLOCK/BMAL1.

[*Keywords*: BMAL1; CLOCK; circadian clock; circadian rhythm; phosphorylation; protein phosphatase 4]

Supplemental material is available for this article.

Received May 1, 2021; revised version accepted June 14, 2021.

The mammalian circadian clock is an endogenous, cell-autonomous oscillator that drives daily rhythms in physiology and behavior. Robust circadian rhythms are essential for the temporal coordination of organ functions, and disruption or maladjustment, e.g., due to our modern lifestyle, is highly associated with various common diseases (Finger et al. 2020; Finger and Kramer 2021). The fundamental mechanism of circadian rhythm generation is a delayed negative transcriptional-translational feedback loop, in which transcriptional repressors (primarily PER and CRY proteins) inhibit their own transcription by precisely controlling the activity of their activators CLOCK/BMAL1 (or NPAS2/BMAL1). For that purpose, both the beginning and end of CLOCK/BMAL1 transcriptional activity are regulated at various levels. For example, control is executed on the timing of (1) nuclear abundance of the transcription factors and their negative regulators, (2) complex formation of the CLOCK/BMAL1 transcription factor heterodimer, (3) DNA binding of the heterodimer (including chromatin structure), and (4) binding of coactivators (e.g., CBP/p300) or inhibitors of transcriptional activity (e.g., PERs, CRYs, and others). Various interdependent steps and interconnected loops govern these regulations, essentially all of which involve post-translational modifications (PTMs) with phosphorylation playing a key role.

All major clock proteins are extensively phosphorylated on Ser/Thr residues (Vanselow et al. 2006; Vanselow and Kramer 2007; Reischl and Kramer 2011; Hirano et al. 2016; Narasimamurthy and Virshup 2021); however, our knowledge about the number, timing, exact location as well as the functional consequence of in vivo phosphorylated amino acids is still limited. In early models, phosphorylation of the negative elements (PER and CRY proteins) was considered to govern the delay between their production and autoinhibition necessary to generate oscillations. Phosphorylation-induced degradation was believed not only to slow down the accumulation of active

[4]**These authors contributed equally to this work.**
Corresponding author: achim.kramer@charite.de
Article published online ahead of print. Article and publication date are online at http://www.genesdev.org/cgi/doi/10.1101/gad.348622.121.

inhibitory complexes and thus contribute to the delay, but would essentially also end the inhibitory action of the PERs and CRYs by removing them entirely. Indeed, the degree of PER and CRY protein phosphorylation is correlated with its abundance, and inhibiting CK1ε/δ (the major PER kinase) activity both stabilizes PER proteins and lengthens the circadian rhythm period. Thus, the phosphorylation-controlled stability of negative regulators (PER and CRY proteins) was considered to be the key determinant for circadian period.

Recent models, however, not only include additional roles of phosphorylation events but also question the cause-and-effect relation between stability of negative elements and circadian period. First, phosphorylation also regulates nuclear import and export of negative regulators PERs and CRYs as well as positive regulators CLOCK and BMAL1 (Tamaru et al. 2009; Yoshitane et al. 2009). Second, phosphorylation controls the heterodimerization, DNA binding, transcriptional activity as well as stability of BMAL1 and CLOCK (Yoshitane and Fukada 2021). For example, CLOCK is phosphorylated in vivo at Ser38 and Ser40, and mutating these residues to Asp (mimicking constitutive phosphorylation) suppresses the transactivation ability of CLOCK (Yoshitane et al. 2009). On the other hand, rhythmic phosphorylation of CLOCK residues S440, S441, and S446 coincides with maximal CLOCK/BMAL1 transcriptional activity, and their mutation to Ala (mimicking a nonphosphorylated state) attenuates transactivation (Robles et al. 2017). In addition, hyperphosphorylation of CLOCK and BMAL1 is correlated with transcriptional activity but also instability. For example, the classical *Clock* mutation (King et al. 1997), which leads to a deletion of 51 amino acids, renders CLOCK hypophosphorylated, more stable, and less transcriptionally active, although dimerization to BMAL1 and binding to DNA is unperturbed (Gekakis 1998; Yoshitane et al. 2009). A possible reason for this is the lack of the binding site for CIPC (Zhao et al. 2007), another negative regulator of CLOCK/BMAL1, which promotes CLOCK phosphorylation (Yoshitane et al. 2009). Moreover, CLOCK phosphorylation is associated with its removal from DNA in the PER/CRY-mediated repression phase, and CK1δ thereby plays an important role (Aryal et al. 2017; Cao et al. 2021). Third, phosphorylation of negative elements does not always promote degradation by creating a recognition site ("phosphodegron") for E3-ubiquitine ligases. For example, CK1ε/δ-mediated phosphorylation at the FASP (familial advanced sleep phase) region of PER2, a series of five serine residues, increases the stability of PER2 and also seems to decrease the activity of CK1ε/δ toward the destabilizing region of PER2. Thus, although PER2 stability seems to be governed by the relative degree of phosphorylation at these two important sites ("phosphoswitch" model) (for review, see Narasimamurthy and Virshup 2021), stability of negative elements may only be correlated with but not cause circadian period length (Kramer 2015; Larrondo et al. 2015). Together, these few examples underline the complexity and pervasiveness of circadian rhythm regulation by Ser/Thr phosphorylation events (for more extensive reviews, see Reischl and Kramer 2011; Hirano et al. 2016; Narasimamurthy and Virshup 2021).

Given the importance of phosphorylation for circadian dynamics, it is rather surprising how little we know about the opponents of the kinases—the phosphatases—within the mammalian circadian oscillator (Reischl and Kramer 2011), although PPP1 (Gallego et al. 2006; Lee et al. 2011; Schmutz et al. 2011) and PPP5 (Partch et al. 2006) have been suggested to modulate circadian dynamics. The phosphorylation state of a Ser/Thr residue is usually precisely controlled by the complex action of both kinases and phosphatases. While >500 genes in the human genome encode for serine/threonine kinases, only about 40 genes encode for serine/threonine phosphatases of the two major families; i.e., phosphoprotein phosphatases (PPPs) and the metal-dependent protein phosphatases (PPMs) (Brautigan and Shenolikar 2018). In addition, kinases are well-studied enzymes with a conserved catalytic domain, while phosphatases are less understood and their substrate specificity and activity is controlled by associated regulatory subunits. In addition, while the presence of a phosphorylated protein residue is unequivocal evidence for the activity of a kinase, its absence is not evidence for the activity of a phosphatase. Thus, it seems plausible that the role of protein phosphatases for circadian rhythm generation is not negligible but merely understudied.

Here, we performed a systematic genetic screen in human U-2 OS cells for Ser/Thr phosphatases of the PPP family essential for normal circadian rhythm generation. We identified protein phosphatase 4 (PPP4C) and its regulatory subunit PPP4R2 as critical for circadian dynamics both in mammalian cells and in *Drosophila*. PPP4 genetic depletion shortens the circadian period, while overexpression lengthens it. PPP4 inhibits CLOCK/BMAL1 transactivation activity likely by binding to BMAL1 and delaying its phosphorylation. This leads to increased CLOCK/BMAL1 DNA occupancy and less transcriptional activity counteracting the "kamikaze" properties of CLOCK/BMAL1. By this mechanism, PPP4 contributes to the critical delay in negative feedback by retarding the PER/CRY/CK1δ-mediated inhibition of CLOCK/BMAL1.

Results

Protein phosphatase 4 (PPP4) is essential for normal circadian rhythms

To identify phosphatases important for circadian rhythm generation, we systematically used RNAi to knock down the catalytic subunits of all known Ser/Thr phosphatases of the PPP family in human U-2 OS cells—an established cell model for peripheral circadian clocks—that harbor a 0.9-kb fragment of the *Bmal1* promoter driving firefly luciferase expression (Maier et al. 2009). While depleting individual catalytic subunits of *PPP1*, *PPP2*, *PPP3*, *PPP5*, *PPP6*, and *PPP7* had no or only subtle effects on circadian period in synchronized U–2 OS reporter cells (Fig. 1A), simultaneous knockdown of several subunits did result in circadian phenotypes (Supplemental Fig. S1A,B), suggesting redundancy among the different catalytic

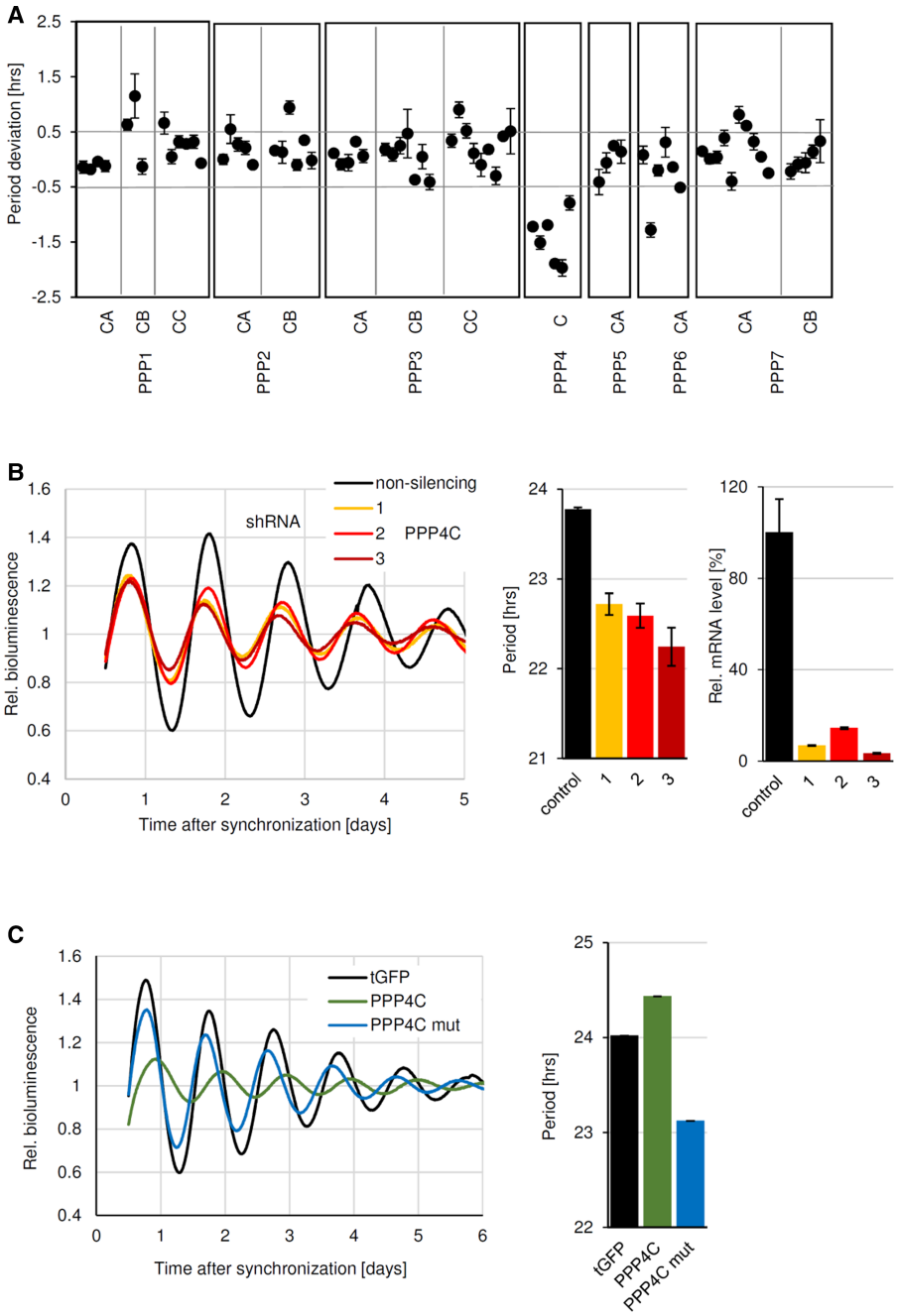

Figure 1. Protein phosphatase 4 (PPP4) is essential for normal circadian rhythms. (*A*) RNAi-based screen for catalytic subunits of all known Ser/Thr-phosphatases important for circadian dynamics. Human U-2 OS cells harboring a Bmal1-luciferase reporter construct were lentivirally transduced with three to 10 shRNA constructs per indicated catalytic subunit, synchronized with dexamethasone, and monitored for 5–7 d in a luminometer. Shown is the mean period deviation (±SD) from nonsilencing controls of three independent experiments performed in a 96-well plate format. (*B*) Trend-eliminated oscillation dynamics of U-2 OS reporter cells lentivirally transduced with shRNA constructs targeting the catalytic subunit of protein phosphatase 4 (PPP4C). Knockdown efficiency was quantified using qPCR. Shown are results from three experiments (mean ± SD). (*C*) Trend-eliminated oscillation dynamics of U-2 OS reporter cells lentivirally transduced with expression constructs for PPP4C, a dominant-negative variant of PPP4C (PPP4C mut), or tGFP as an overexpression control. Shown are results from three experiments (mean ± SD).

subunits. In contrast, silencing the catalytic subunit of protein phosphatase 4 (*PPP4C*) consistently (five different shRNA constructs) and robustly shortened the circadian period by up to ~1.5 h (Fig. 1A,B). Period shortening upon *PPP4C* knockdown also occurred in human astrocytes (U87) as well as in primary mouse fibroblasts, indicating a fundamental role for *PPP4C* in regulating mammalian circadian clocks (Supplemental Fig. S2A).

Furthermore, overexpression of *PPP4C* led to period lengthening and a substantial decrease of circadian amplitude, whereas overexpression of a dominant-negative, catalytically inactive *PPP4C* mutant (Zhou et al. 2002) phenocopied the knockdown and shortened the circadian period (Fig. 1C). Moreover, combining knockdown of endogenous *PPP4C* and overexpression of the catalytically inactive *PPP4C* mutant did not further shorten the circadian period (Supplemental Fig. S2B), together indicating that PPP4C level and in particular its catalytic activity are essential for normal circadian rhythms.

CLOCK/BMAL1-mediated transcription may be a target of PPP4 activity

To gain insight into the molecular basis of *PPP4C*'s modulation of circadian rhythms, we quantified the transcript levels of clock genes upon *PPP4C* depletion in synchronized U-2 OS cells harvested at regular 4-h intervals over about two circadian cycles. While we could clearly see the advanced phase of clock gene transcript rhythms (probably due to the short period upon *PPP4C* depletion), we did not see any substantial effect on the overall abundance of most clock gene transcripts (Fig. 2A). An exception was *BMAL1*, whose mRNA levels were reduced at all circadian phases, similar to the *Bmal1*-luciferase-derived bioluminescence, which is a proxy for *BMAL1* promoter activity. Despite the lower *BMAL1* transcript levels, target genes of the CLOCK/BMAL1 transcription factor, such as *DBP*, *PER3*, or *NR1D1* did not show reduced transcript levels, which may suggest (among other possibilities) that CLOCK/BMAL1 is more active in *PPP4C*-depleted cells. Overexpression of *PPP4C*, however, has a more severe effect on clock gene transcript levels: Besides the reduced amplitude already seen in the bioluminescence experiments (Fig. 1C), target genes of CLOCK/BMAL1 with important E-boxes in their promoters such as *DBP*, *PER3*, or *NR1D1* showed substantially reduced transcript levels (Fig. 2B). Note that, e.g., *DBP* levels are anticorrelated with *PPP4C* levels, which decrease over time. Together, these findings suggest that CLOCK/BMAL1-mediated transcription is modulated by PPP4C activity.

PPP4C acts negatively on CLOCK/BMAL1 transactivational activity

Two mutually not exclusive hypotheses could explain our findings so far: (1) PPP4 acts positively on *BMAL1* transcription, and (2) PPP4 acts negatively CLOCK/BMAL1-mediated transcription. The first hypothesis is supported by the fact that mean *BMAL1* levels were low upon *PPP4C* depletion (Fig. 2A); the second hypothesis is backed by the finding that PPP4C overexpression was correlated with low transcript levels of typical E-box-containing CLOCK/BMAL1 target genes. We found no convincing evidence further supporting the first hypothesis (Supplemental Fig. S3; Supplemental Material). To test the second hypothesis, i.e., that PPP4C acts negatively on E-box-mediated transcription, we performed a transactivation assay in HEK293 cells with a reporter construct that expresses luciferase under the control of six tandem E-boxes. As expected, coexpression of CLOCK/BMAL1 increased the luciferase signal and the known repressor CRY1 substantially reduced it. While expression of PPP4C had no effect on the reporter alone, coexpression of PPP4C, but not the catalytically inactive mutant, inhibited the transactivational activity of CLOCK/BMAL1 to about 50%, indicating that PPP4 activity can modulate CLOCK/BMAL1 transcriptional activity (Fig. 3A). To test whether PPP4C is acting on CLOCK or BMAL1, we have replaced CLOCK by NPAS2 or CLOCKΔ19 that lacks 51 residues encoded by exon 19 that are crucial for normal transactivation (Gekakis 1998). In both cases, coexpression of PPP4C persisted to inhibit the transactivation properties of the heterodimer to about 50% (Fig. 3B), indicating that CLOCK itself is probably not a direct target of PPP4C but possibly BMAL1 or transcriptional cofactors.

PPP4R2 is the regulatory subunit crucial for normal rhythms in human cells and Drosophila

Protein phosphatase 4 holoenzyme consists of one catalytic subunit and one regulatory subunit; the latter is believed to confer substrate specificity (Cohen et al. 2005). To learn more about the PPP4 substrate(s) modulating circadian dynamics, we systematically searched for the corresponding PPP4 regulatory subunit. To this end, we depleted all known PPP4 regulatory subunits using RNAi in oscillating U–2 OS cells and identified PPP4R2 as the only subunit, which also led to short period rhythms upon silencing (Fig. 4A). This phenotype was robust and reproducible for several RNAi constructs and its extent was similar to PPP4C knockdown (~1.5-h period shortening) (Fig. 4B). Importantly, overexpression of PPP4R2 also lengthened the circadian period (Supplemental Fig. S4A), and simultaneous depletion of both the catalytic as well as the regulatory subunit did not further shorten the circadian period (Supplemental Fig. S4B). In addition, while PPP4R2 alone could not suppress CLOCK/BMAL1 activity in HEK293 cells, simultaneous expression with PPP4C led to a stronger inhibition than PPP4C alone (Supplemental Fig. S4C). Together, these data indicate that PPP4C and PPP4R2 form the PPP4 holoenzyme essential for normal circadian dynamics likely by modulating CLOCK/BMAL1 transactivational activity.

Does protein phosphatase 4 also play a role in invertebrates? To test this, we studied behavioral rhythms in *Drosophila* upon knockdown of the expression of PPP4R2r (the homolog to mammalian PPP4R2). We used two independent UAS-PPP4R2r-RNAi lines targeting different regions of the PPP4R2r mRNA to minimize potential off-target effects. Using the binary Gal4/UAS system (Brand and Perrimon 1993), we down-regulated PPP2R2r in all clock cells with a *timeless-Gal4* driver (Kaneko and Hall 2000) or in the subset of the brain pacemaker neurons expressing the neuropeptide PDF with *Pdf-Gal4* (Renn et al. 1999). Flies with PPP4R2r knockdown in all clock cells were robustly rhythmic in constant darkness with periods ~1 h shorter compared with the control flies (Fig.

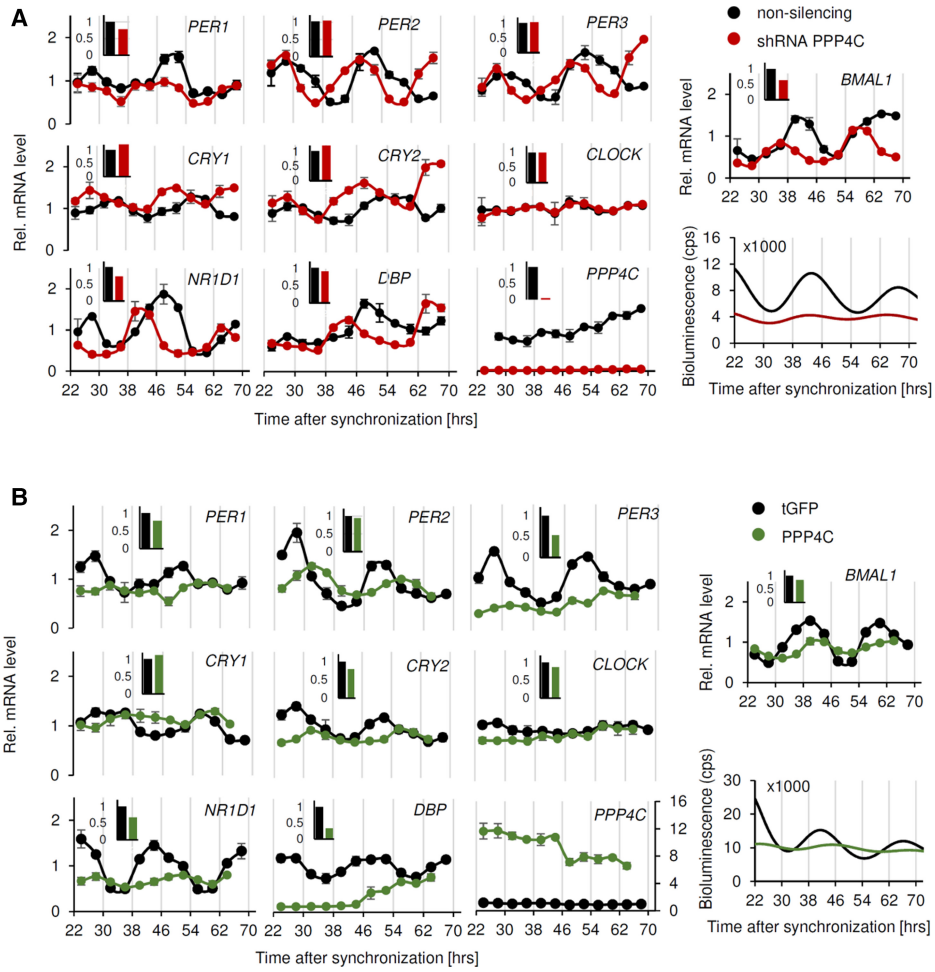

Figure 2. Protein phosphatase 4 gene dosage modulates clock gene expression. (*A*) Human U-2 OS cells were lentivirally transduced with a nonsilencing control (black) or an shRNA construct targeting PPP4C (red) and harvested for total RNA preparation in 4-h intervals starting 24 h after dexamethasone synchronization. Expression of indicated genes was quantified using qPCR and normalized to *GAPDH* expression. Shown are results from three experiments (mean ± SD). *Inset* bar diagrams visualize mean expression over all time points of the time series. (*Bottom right*) Raw bioluminescence data of *Bmal1*-luciferase reporter cells for comparison. (*B*) Human U-2 OS cells were lentivirally transduced with expression constructs for tGFP (as control, black) or for PPP4C (green) and harvested for total RNA preparation in 4-h intervals starting 24 h after dexamethasone synchronization. Expression of indicated genes was quantified using qPCR and normalized to *β-Actin* expression. Shown are results from three experiments (mean ± SD). *Inset* bar diagrams visualize mean expression over all time points of the time series. (*Bottom right*) Raw bioluminescence data of *Bmal1*-luciferase reporter cells for comparison.

4C,D; Supplemental Fig. S5A; Supplemental Table S1). More restricted knockdown in the PDF neurons had only a small effect on period length (Fig. 4D), and period shortening was not significant when compared with the RNAi lines not expressing the *Pdf-Gal4* driver (Supplemental Table S1; Supplemental Fig. S5B). This indicates that PPP4R2r also controls clock speed in non-PDF clock neurons, or that the RNAi-mediated knockdown in the PDF neurons was more efficient with the *tim-Gal4* driver compared with *Pdf-Gal4*. Next, we overexpressed PPP4R2r using a fly line with an UAS insertion immediately upstream of the *PPP4R2r* gene (EP307). Overexpression with *tim-Gal4* and *Pdf-Gal4* led to mild but significant period lengthening of 0.2 h–0.6 h compared with controls (Fig. 4C,D; Supplemental Table S1; Supplemental Fig. S5C). In summary, the results show that, both in mammalian cells and in *Drosophila*, PPP4R2r influences circadian clock speed in the same direction.

PPP4 interacts with BMAL1 and is rhythmically expressed

If BMAL1 is a direct target of PPP4, it might be possible to detect an interaction with PPP4, although enzyme-substrate interactions are expected to be transient. To test this, we performed coimmunoprecipitation experiments in HEK293 cells ectopically expressing a BMAL1-luciferase fusion protein using antibodies against endogenous PPP4C and PPP4R2. As a positive control, we used an antibody against endogenous CRY1, a known interaction

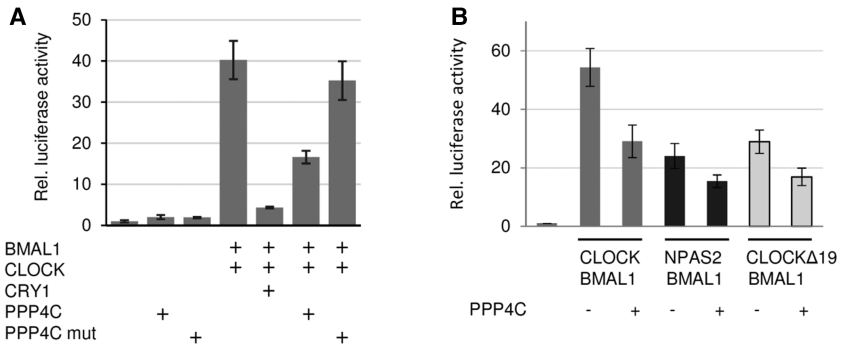

Figure 3. PPP4C acts negatively on CLOCK/BMAL1 transactivational activity. (*A*) CLOCK/BMAL1-mediated transactivation from six E-boxes containing luciferase construct in HEK293 cells. Indicated expression constructs were cotransfected. Shown are means ± SD from three independent samples. (*B*) Transactivation from reporter construct as described in *A* with CLOCK, NPAS2, or CLOCKΔ19 (missing 51 residues corresponding to exon 19) as partners for BMAL1 ($n = 6$, mean ± SD).

partner of BMAL1, which resulted in approximately threefold more luciferase activity in the precipitate than the negative control (IgG only). The anti-PPP4R2 antibody led to significant precipitation of BMAL1-luciferase, whereas the anti-PPP4C antibody had only a subtle effect (Fig. 5A).

Next, we asked whether BMAL1 phosphorylation status might be correlated with PPP4 abundance. To test this, we harvested livers at regular 3-h intervals from mice kept in constant dark conditions and performed Western blot experiments using antibodies against PPP4R2 as well as against BMAL1. PPP4R2 protein levels were rhythmic and peaked around CT3 (Fig. 5B), just before maximal CLOCK/BMAL1 binding to their target chromatin sites (CT6-7) (Koike et al. 2012). This is consistent with proteomics data reported by the Naef and Gachon laboratories (Wang et al. 2017) showing that nuclear levels of the PPP4 catalytic subunit are rhythmic with a similar phase (replotted in Fig. 5C). Shortly after PPP4R2 and PPP4C levels decrease, total and nuclear BMAL1 levels also decline (Fig. 5B,C). Interestingly, although BMAL1 is hyperphosphorylated at all times, it is less hypophosphorylated at times when PPP4 levels are low (CT9-12) (Fig. 5B), as also recently reported by the Sancar laboratory (Cao et al. 2021), suggesting that PPP4 may modulate BMAL1 phosphorylation status and activity.

PPP4 modulates the 'kamikaze' properties of CLOCK/BMAL1

CLOCK/BMAL1 has been described to be a so-called kamikaze transcription factor; i.e., it is most active when it is about to be degraded by the ubiquitin-proteasome system (Kondratov 2003; Sahar et al. 2010; Stratmann et al. 2012). For example, inhibition of the proteasome prolonged the (highly stochastic) residence time of CLOCK/BMAL1 on the *Dbp*-promoter but simultaneously suppressed *Dbp* transcription (Stratmann et al. 2012). In fact, for kamikaze transcriptional activators there is a correlation between activity and instability. Post-translational modifications, such as phosphorylation, sumoylation, and ubiquitination play key modulatory roles in this context (Thomas and Tyers 2000; Tansey 2001). Thus, if PPP4 alters the activity of CLOCK/BMAL1 by influencing its kamikaze properties, the following predictions arise: (1) effects of PPP4 activity on circadian dynamics may depend on proteasome activity, and (2) depleting PPP4 should reduce the CLOCK/BMAL1 occupancy on its target promoters.

To test the first prediction, we treated U–2 OS cells (either control or *PPP4C*-depleted) with increasing concentrations of the proteasomal inhibitor MG132. We found that in PPP4C-depleted cells, the 1.5-h period shortening (due to *PPP4C* silencing) was lost upon treatment with higher concentrations of MG132, while such MG132 concentrations had no effect on control cells (Supplemental Fig. S6), suggesting that proteasomal function and PPP4 activity work together to determine the circadian period.

To test the second prediction, we conducted two sets of experiments. We first performed anti-BMAL1 chromatin immunoprecipitation in *PPP4C*- and *PPP4R2*-depleted as well as in control cells at two different circadian times (24 h and 36 h after synchronization) and measured BMAL1 occupancy on the *NR1D1* promoter by quantitative PCR. As described previously (e.g., Ripperger and Schibler 2006; Koike et al. 2012), BMAL1 binding is dependent on circadian phase; i.e., it is substantially higher at 24 h compared with 36 h after synchronization. Importantly, although total nuclear abundance of BMAL1 was unaffected in both *PPP4C*- and *PPP4R2*-depleted cells (Supplemental Fig. S7), BMAL1 chromatin occupancy was reduced to about 50% at the time of maximal transcription (24 h after synchronization) but not when BMAL1 binding was minimal (Fig. 6A). This indicates that PPP4 indeed regulates BMAL1 occupancy on its target genes.

The second set of experiments was inspired by work from the Schibler laboratory (Stratmann et al. 2012). They created an NIH3T3 mouse fibroblast cell line that harbors a tandem array of the *Dbp* gene in the genome, which enabled them to monitor the binding of BMAL1 (fused to the fluorescent reporter protein YFP) to this array by time-lapse microscopy. The diffusion kinetics of BMAL1-YFP served as a readout for chromatin binding. We also used these cells, down-regulated *PPP4R2,* and performed fluorescence recovery after photobleaching (FRAP) experiments, in which we bleached the fluorescence of the nuclear spots (representing BMAL1-YFP binding to the *Dbp*-array). Our first observation was that the number of detectable spots was reduced in *PPP4R2*-depleted cells compared with control cells (Supplemental Fig. S8). Our second observation was that, in *PPP4R2*-depleted cells, the fluorescent recovery after photobleaching

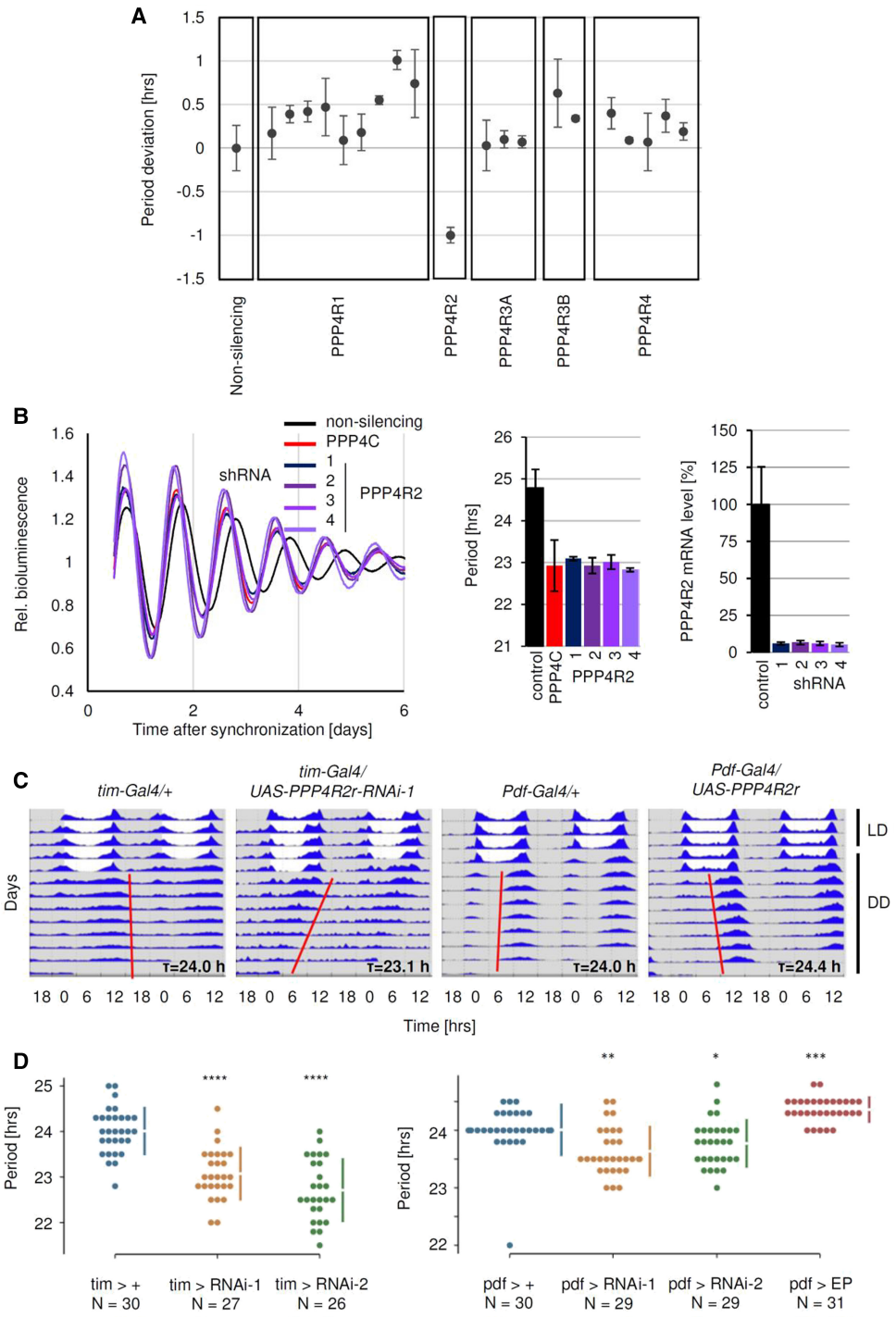

Figure 4. PPP4R2 is the PPP4 regulatory subunit crucial for normal rhythms in human cells and *Drosophila*. (*A*) RNAi-based screen for all known PPP4 regulatory subunits important for circadian dynamics. Human U-2 OS cells harboring a *Bmal1*-luciferase reporter construct were lentivirally transduced with one to nine shRNA constructs per indicated catalytic subunit (number depended on availability in our laboratory RNAi construct library), synchronized with dexamethasone, and monitored for 5–7 d in a luminometer. Shown is the mean period deviation (±SD) from nonsilencing controls of three independent experiments performed in a 96-well plate format. (*B*) Trend-eliminated oscillation dynamics of U-2 OS reporter cells lentivirally transduced with shRNA constructs targeting the regulatory subunit of protein phosphatase 4, PPP4R2. Knockdown efficiency was quantified using qPCR. Shown are results from three to five experiments (mean ± SD). (*C*) Double-plotted actograms showing behavioral activity of male flies of the indicated genotype during LD (days 1–5) and DD (days 6–12) at constant 25°C. The *tim-Gal4:27* line used here also contains the *UAS-Dicer* construct to enhance RNAi efficiency. For overexpressing *PPP4R2r*, the *P{EP}PPP4R2r*^{EP307} line with an *UAS* insertion immediately upstream of the transcription start site was employed. (*D*) Statistical analysis of differences between control flies and those down-regulating or overexpressing *Drosophila PPP4R2r*. The individual period values of the indicated genotypes are plotted. The mean ± SD are shown as vertical colored lines and the mean is indicated as a gap in the line. (RNAi-1) *UAS-PPP4R2r-RNAi TRiP BL26296*, (RNAi-2) *UAS-PPPR2r v105399/+*, (tim) *tim-gal4:27 UAS-Dicer*, (Pdf) *Pdf-gal4*, (EP) *P{EP}PPP4R2r*^{EP307}. *P*-values were determined by Student's *t*-test: (****) $P < 0.00005$, (***) $P < 0.0005$, (**) $P < 0.005$, (*) $P < 0.05$.

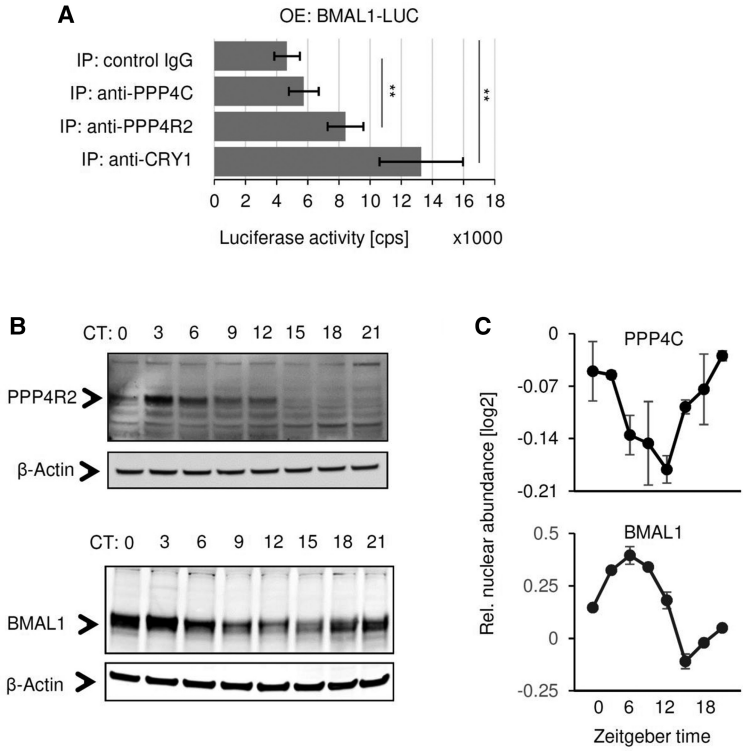

Figure 5. PPP4 interacts with BMAL1 and is rhythmically expressed. (*A*) Coimmunoprecipitation experiments with lysates from HEK293 cells expressing a BMAL1-luciferase fusion protein. Shown are mean luciferase activity counts after precipitation with specific anti-CRY1, anti-PPP4R2, anti-PPP4C antibodies or unspecific IgG control antibody (mean ± SD, $n = 3$ independent IPs). Student's *t*-test: (**) $P < 0.01$. (*B*) Western blots with anti-PPP4R2 and anti-BMAL1 antibodies (and anti-β-Actin antibody as loading control) from liver lysates harvested from mice at the indicated circadian times. (*C*) Replotted data from a proteomics study performed by Wang et al. (2017). Shown are nuclear abundances of PPP4C and BMAL1 over the course of 1 d. Error bars represent SEM between two biological replicates.

was substiantially slower and never reached the level of control cells (Fig. 6B; Supplemental Movies S1, S2), indicating that BMAL1-YFP could not accumulate efficiently at the *Dbp* promoter.

Taken together, these data suggest that the effect of PPP4 on the circadian clockwork likely occurs through modulation of CLOCK/BMAL1 activity, stability, and target binding, properties that are mutually dependent.

Discussion

From cyanobacteria to humans, rhythmic post-translational modifications are essential design principles in all known circadian clock mechanisms. In this context, phosphorylation of clock proteins are key processes and have been studied for >25 yr following the discovery of rhythmic PER protein phosphorylation in *Drosophila* (Edery et al. 1994). Surprisingly, however, the majority of studies dealt with the phosphorylation step by kinases and not with its counterpart—dephosphorylation by phosphatases—although reversible protein phosphorylation is considered a major control mechanism for essentially all aspects of cell physiology.

To shed light on this little understood aspect of circadian regulation, we performed a systematic RNA interference screen to identify Ser/Thr phosphatases essential for circadian rhythmicity in mammalian cells. Both, the catalytic subunit of protein phosphatase 4 and one of the associated regulatory subunits (PPP4R2) turned out to be required for normal circadian rhythms in several mammalian cell types. Knockdown resulted in short period rhythms, and overexpression resulted in long period rhythms in both mammalian cells and living *Drosophila*, indicating a universal role for PPP4 in animal clocks. The mechanism of PPP4 action on the mammalian molecular clock is that it inhibits CLOCK/BMAL1 transactivation activity, probably by dephosphorylating BMAL1, leading to its sustained target gene binding and increased stability. By this mechanism, PPP4 counteracts the kamikaze properties of CLOCK/BMAL1 and delays the PER/CRY/CK1δ-mediated inhibition (Cao et al. 2021).

We have not been able to identify specific BMAL1 phosphorylation sites that are dephosphorylated by PPP4. In the nucleus, CLOCK and BMAL1 are codependently hyperphosphorylated (Lee et al. 2001; Kondratov 2003). Probably most in vivo phosphorylation sites are yet unmapped and most corresponding kinases (and phosphatases) are unassigned, although in vitro CK1ε, GSK3β, and PKCα as well as members of the MAPK family are able to phosphorylate BMAL1, while PKG, PKCα/γ, and GSK3β can phosphorylate CLOCK (for review, see Yoshitane and Fukada 2021).

Two recent studies point to a prominent role of CK1δ as a potential CLOCK/BMAL1 kinase. First, CK1δ is present in the multiprotein PER-CRY repressor complex in mouse livers, which is rhythmically recruited to inhibit CLOCK/BMAL1 transcription activity (Aryal et al. 2017). Second, CK1δ promotes the dissociation of CLOCK-BMAL1 from its target promoters likely by phosphorylation of CLOCK (Cao et al. 2021). Thus, it becomes increasingly plausible that the phosphorylation status of CLOCK/BMAL1 is a major determinant of its activity. A link between transcriptional activation and phosphorylation (and subsequent ubiquitination and degradation) is common to many unstable transcription

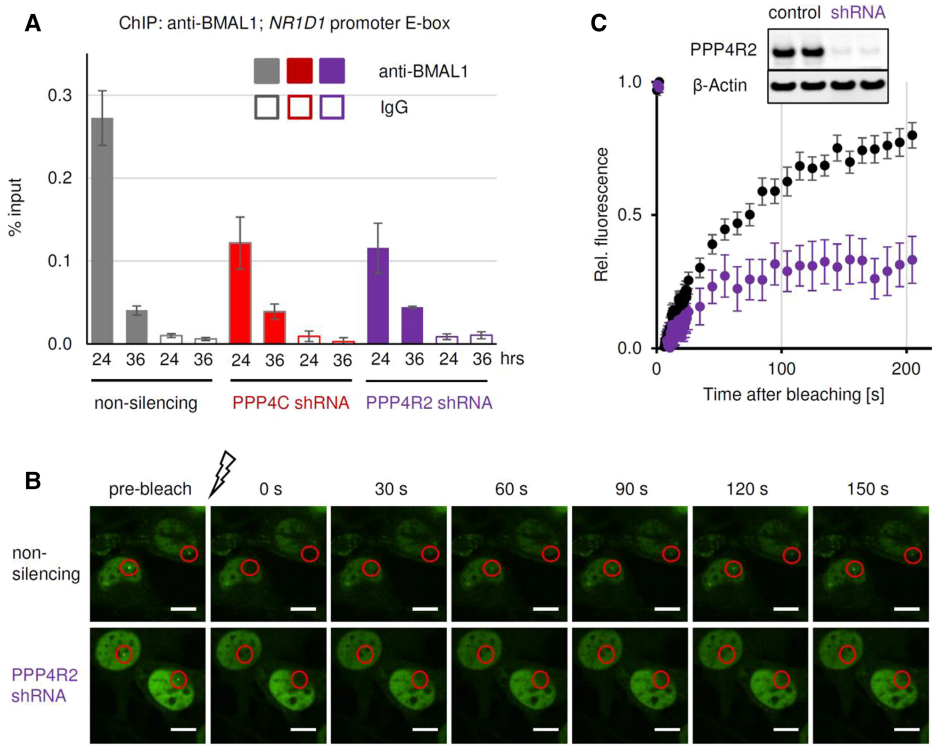

Figure 6. CLOCK/BMAL1 occupancy on target promoters is modulated by PPP4. (*A*) Chromatin immunoprecipitation experiments with anti-BMAL1 antibody (or control IgG) performed in synchronized U-2 OS cells lentivirally transduced with shRNA constructs targeting the catalytic (PPP4C) or regulatory PPP4R2 subunit of protein phosphatase 4. Chromatin was harvested 24 and 36 h after dexamethasone synchronization, and BMAL1 presence on *NR1D1* promoter was analyzed via qPCR. Shown are results from five independent precipitations (mean ± SD). (*B*) Kinetics of BMAL1-YFP binding to *Dbp* gene arrays in murine NIH3T3 cells (Stratmann et al. 2012) was analyzed using fluorescence recovery after photobleaching (FRAP) experiments. Shown are representative fluorescence microscopy images of control or PPP4R2-depleted cells before and after photobleaching of BMAL1-YFP located at the *Dbp* gene arrays (visible as bright spots). Scale bar, 10 µm. (*C*) Quantification of FRAP experiments described in *B*. Given are mean (±SEM) relative fluorescence intensities after photobleaching for 25 cells (*Ppp2r2* knockdown) and 47 cells (nonsilencing control).

factors and has been proposed as "black widow" (Tansey 2001) or "kamikaze activator" models (Thomas and Tyers 2000) for CLOCK/BMAL1 (Kondratov 2003; Kwon et al. 2006; Stratmann et al. 2012). According to those models, kinases as well as ubiquitin ligases are recruited to the transcription factors by the basal transcription machinery, mono-ubiquitination of phosphorylated transcription factors license them for transactivation and subsequently promote rapid polyubiquitination and degradation.

In fact, proteasomal inhibition not only prolongs the retention time of CLOCK/BMAL1 on DNA, which normally fluctuates stochastically with a timescale of minutes resulting in transcriptional bursts, but also attenuates E-box-dependent transcription (Stratmann et al. 2012). This is consistent with our finding that proteasomal inhibition blocks the effect of PPP4 down-regulation on circadian period. Moreover, we found DNA occupancy and retention time of CLOCK/BMAL1 decreased upon PPP4 down-regulation. Together, this suggests that PPP4 counteracts the phosphorylation-mediated activation, destabilization, DNA removal, and subsequent proteasomal degradation of CLOCK/BMAL1.

Also, in fungal circadian clocks (e.g., in *Neurospora crassa*), phosphorylation of heterodimeric activators (WC-1 and WC-2) is correlated with rhythmic inhibition. As in animal clocks, the negative element (FRQ) brings kinases (e.g., CK1), which not only phosphorylates the negative element but also the WC-1–WC-2 complex at >90 sites, resulting in transactivational inhibition and removal from DNA (He and Liu 2005; Schafmeier et al. 2005; He et al. 2006; Wang et al. 2019). Thus, phosphorylation of positive elements by kinases recruited by negative elements seems to be a common design principle of circadian clocks.

Protein phosphatase 4 (PPP4) is a ubiquitously expressed serine/threonine phosphatase modulating many cellular functions, including organelle assembly (centrosome and splicosome), cellular signaling (NFκB and TOR pathways), spermatogenesis, DNA damage response, and regulation of chromatin activities (via regulation of HDAC3 activity) (for review, see Cohen et al. 2005). In addition, PPP4 has been linked to glucose metabolism and TNF-α-induced hepatic insulin resistance, and its levels have been shown to be elevated in the type 2 diabetes mouse model (db/db) (Zhao et al. 2015). A role for PPP4

within the circadian clock was unknown so far, although during an RNAi screen the Hardin laboratory found first indications for PPP4R2r possibly being important for circadian rhythms in *Drosophila* (Agrawal and Hardin 2016). Given the known interplay between circadian and metabolic pathways (Finger et al. 2020), it is tempting to speculate that some of the circadian phenotypes observed in mice with metabolic dysfunctions are mediated by PPP4. Indeed, the disruption of circadian behavioral activity observed in db/db mice (Grosbellet et al. 2016) could be caused by increased PPP4 expression (Zhao et al. 2015), which, at least in our cell model, resulted in a substantial reduction in circadian amplitude.

Our RNAi screen also uncovered potential roles for other phosphatases, such as PPP1, PPP2, PPP3, and PPP7. Depleting individual catalytic subunits of those phosphatases had no or only subtle effects on circadian rhythms, but a simultaneous knockdown of several catalytic subunits did result in circadian phenotypes suggesting redundancy among the different catalytic subunits. Depleting PPP1 subunits lengthened the circadian period in agreement with previous results by Schmutz et al. (2011), while coknockdown of PPP2, PPP3 and PPP7 catalytic subunits substantially reduced the amplitude of circadian rhythms. More work is needed to elucidate the molecular targets of these phosphatases.

In summary, this study sheds light on the much less studied counterregulation of phosphorylation, the dephosphorylation events, and identifies PPP4 as a novel player within the circadian clockwork of mammals and *Drosophila*. PPP4's main action is on the CLOCK/BMAL1 complex; it primarily regulates its activity by modulating its DNA occupancy. Further work is needed to identify the exact sites on BMAL1 (and maybe CLOCK) that are dephosphorylated by PPP4 to get even more mechanistic insight into the molecular basis of circadian rhythm generation. Our study is the first step.

Materials and methods

RNAi-mediated knockdown and overexpression

RNAi constructs were purchased from Open Biosystems. Lentiviruses were produced in HEK293T cells in a 96-well plate format essentially as described (Maier et al. 2009; Maier et al. 2021). Virus-containing supernatants were filtered and U-2 OS (human; American Type Culture Collection [ATCC] HTB-96) reporter cells or NIH3T3 *Dbp* gene array cells (Stratmann et al. 2012) were transduced with 100 µL of the virus filtrate plus 8 ng/µL protamine sulfate. After 1 d, the medium was replaced with medium containing 10 µg/mL puromycin before bioluminescence recording. For overexpression of protein phosphatase 4 subunits in U–2 OS reporter cells, cells were lentivirally transduced with the respective expression constructs in 35-mm dishes essentially as described (Maier et al. 2009). After 3 d, medium was exchanged to 5 µg/mL blasticidine selective medium.

Bioluminescence imaging

U-2 OS cells (human; ATCC HTB-96) stably expressing firefly luciferase from a *Bmal1* promoter fragment (Maier et al. 2009) and U87 (human; ATCC HTB-14) stably expressing a *Per2*-luciferase reporter construct or primary PER2-LUC fibroblasts (isolated from ear tissue of reporter mice) (Yoo et al. 2004) were seeded either onto a white 96-well plate (2×10^4 cells/well) or in 30-mm NUNC dishes (2×10^5 cells/well). After 72 h, cells were synchronized with 1 µM dexamethasone for 30 min, washed with PBS, and cultured in Phenol-Red-free DMEM containing 10% fetal bovine serum, antibiotics (100 U/mL penicillin, 100 µg/mL streptomycin), and 250 µM D-luciferin (Biothema). For pharmacological treatments, the indicated MG-132 (Calbiochem) concentrations were added. Bioluminescence recordings were performed at 35°C–37°C in a 96-well plate luminometer (TopCount, PerkinElmer) or LumiCycle (Actimetrics). Data were analyzed using ChronoStar software as described previously (Maier et al. 2021).

Quantitative RT-PCR

Cells were harvested either 24 h after synchronization with 1 µM dexamethasone for 30 min or upon termination of bioluminescence recordings. Total RNA was prepared using a Pure Link RNA mini kit (Life Technologies) according to the manufacturer's protocol and then reverse-transcribed to cDNA using M-MLV reverse transcriptase (Life Technologies). Quantitative PCR was performed with SYBR Green fluorescence assays and analyzed in a CFX96 machine (Bio-Rad). For quantitative PCR, QuantiTect primers (Qiagen) were used, except for human *GAPDH* (hGAPDH_fwd: TGCACCACCAACTGCTTAGC; hGAPDH_rev: ACAGTCTTCTGGGTGGCAGTG), mouse Gapdh (mGAPDH_fwd: AAAGCTCACTGGCATGGCCTTGGGC; mGAPDH_rev: CATGAGGTCCACCACCCTGTTGCTG), and the 3′ UTR of PP P4C (hPPP4C_3′_UTR_fwd: CAAGAGGGTGCTTCGAGGGT; hPPP4C_3′_UTR_rev: GGTTCAAGTGGGGAGAGAGG). The transcript levels were normalized to Gapdh and evaluated according to the $2^{\Delta\Delta Ct}$ method.

Luciferase reporter assay

HEK293 cells (human, ATCC CRL-1573, regularly tested for mycoplasma) were seeded in 24-well plates in antibiotic-free medium. After reaching 80%–90% confluence, transfection was performed using Lipofectamine 2000 (Life Technologies) according to the manufacturer's protocol. The total amount of transfected DNA in each sample was 1.2 µg, composed of a firefly luciferase reporter construct (50 ng of pGL3/six E-box elements) and 300 ng of mClock, 300 ng of mBmal1, 15 ng of mCry1, 400 ng of PPP4C, 400 ng of PPP4C mut, 400 ng of mCLOCKΔ19, and 400 ng of mNPAS2 or as indicated. For normalization, 2 ng of a *Renilla* luciferase vector pRL-SV40 was cotransfected. The total amount of DNA per well was adjusted to 1.2 µg by adding empty pDEST26 vector. Cells were harvested 48 h after transfection in 200 µL of passive lysis buffer (PLB) and frozen for 1 h at –80°C. Cell lysates were homogenized by vortexing and luciferase activity was measured by using the dual-luciferase reporter assay system (Promega) according to the manufacturer's protocol in a 96-well plate-reading luminometer (Orion II, Berthold Detection System). Five microliters of each cell extract was measured in duplicate by first adding 25 µL of LARII to measure firefly luciferase activity, and then 25 µL of Stop & Glow reagent to detect the renilla luciferase activity. For data analysis, firefly luciferase activity was normalized to the corresponding renilla luciferase activity.

Coimmunoprecipitation

HEK293 cells were lentivirally transduced with a pLenti6 (Invitrogen) construct coding for a BMAL1::LUCIFERASE fusion protein.

Cells were harvested in co-IP buffer (20 mM Tris-HCl at pH 8.0, 140 mM NaCl, 1.5 mM $MgCl_2$, 1 mM TCEP, 1% Triton-X-100, 10% glycerin) containing protease inhibitor cocktail (Sigma-Aldrich P-8340). Input counts of 5 µL of lysate were detected with the Betascout liquid scintillation counter (PerkinElmer) using 25 µL of LARI (Promega) as a substrate-containing reagent for 10 sec. Lysates containing 10 million counts were used for co-IP experiments. Pull-downs were performed with 2 µg each of the following antibodies: anti-PPP4C (Proteintech 10262-1-AP), anti-PPP4R2 (Bethyl A300-838A), in-house anti-CRY1, or an isoform-specific ideotypic antibody (normal rabbit IgG; Santa Cruz Biotechnologies SC-2027) with G Plus agarose beads (Santa Cruz Biotechnologies) via overnight incubation at 4°C under constant agitation. Beads were washed three times in 250 µL of washing buffer (20 mM Tris-HCl at pH 8.0, 150 mM NaCl, 0.5% Igepal CA-630). Luciferase activity of precipitated beads was measured as described for input detection 30 sec after the addition of LARI.

Nuclear extracts from U-2 OS cells

Confluent U-2 OS cells were washed twice with cold 1× PBS. Then, cells were rinsed with cold HLB buffer (20 mM Tris-HCl at pH 7.5, 10 mM NaCl, 3 mM $MgCl_2$) and harvested in HLB buffer containing protease inhibitor cocktail (Sigma-Aldrich P-8340). Cells were mechanically homogenized keeping nuclei intact. Nuclei were pelleted at 3500*g* for 5 min at 4°C. Pellets were washed, and centrifugation and washing were repeated. Nuclei were resuspended in SDS buffer (4% SDS, 10 mM DTT, 100 mM Tris-HCl at pH 7) and kept for 30 min on ice followed by mechanical homogenization. Lysates were centrifuged at 14,000*g* for 20 min at 4°C. Supernatants were considered as nuclear extracts and subjected to Western blot analysis.

Western blot

C57BL/6 mice were entrained to a 12-h light/12-h dark cycle for >14 d. After transfer in constant darkness, animals were sacrificed at indicated circadian time points (CT) for liver extraction. Tissue was lysed in RIPA buffer (1× PBS, 1% Igepal CA-630, 0.5% Na-deoxicholate, 0.1% SDS) containing protease inhibitor cocktail (Sigma-Aldrich P-8340). Proteins were denatured in SDS loading buffer (Invitrogen) for 10 min at 95°C. Separation was performed by SDS-PAGE with 4%–12% Bis-Tris gels (Invitrogen). Proteins were transferred to nitrocellulose membrane, blocked in PBS(T) with 5% nonfat dry milk for 1 h at room temperature, and probed with the antibodies anti-PPP4R2 (Bethyl A300-838A) and anti-BMAL1 (kind gift from Michael Brunner, Heidelberg) overnight at 4°C. Membranes were washed three times for 5 min in PBS(T), and incubated with the corresponding HRP-conjugated secondary antibody (Santa Cruz Biotechnologies SC-2305) for 1 h at room temperature. After three additional washing steps, a chemiluminescence reaction was performed with Super SignalWest Pico substrate (Pierce). Protein bands were visualized using the ChemoCam (Intas) detection system. NIH3T3 *Dbp* gene array cells were lysed in RIPA buffer (1× PBS, 1% Igepal CA-630, 0.5% Na-deoxicholate, 0.1% SDS) containing protease inhibitor cocktail (Sigma-Aldrich P-8340). PPP4R2 protein detection was performed via Western blot as described above using the anti-PPP4R2 (Bethyl A300-838A) antibody. Purity of nuclear extracts was verified using antibodies against Lamin A (H-102; Santa Cruz Biotechnologies sc-20680) and α-Tubulin (B7; Santa Cruz Biotechnologies sc-5286).

Chromatin immunoprecipitation (ChIP)

U-2 OS cells were grown in 20-cm dishes to 95% confluence. Cells were synchronized with 1 µM dexamethasone for 1 h. Cross-linking, chromatin preparation, and chromatin immunoprecipitation were performed at indicated times after synchronization as described (Ripperger and Schibler 2006) with the following modifications. Cells were sonicated on ice five times for 15 sec at a 50% setting, and then centrifuged at 13,000 rpm for 10 min. Supernatants were diluted in buffer (1.1% Triton X-100, 2 mM EDTA, 150 mM NaCl, 20 mM Tris-HCl at pH 8.1), precleared with agarose beads for 1 h at room temperature, and incubated with 2 µg of anti-BMAL1 antibody (kind gift of Michael Brunner, Heidelberg) or normal rabbit IgG (Santa Cruz Biotechnologies SC-2027) and agarose beads for 1 h at room tempterature with rotation. Precipitates were washed sequentially in TSE I (0.1% SDS, 1% Triton X-100, 2 mM EDTA, 20 mM Tris-HCl at pH 8.1, 150 mM NaCl), TSE II (0.1% SDS, 1% Triton X-100, 2 mM EDTA, 20 mM Tris-HCl at pH 8.1, 500 mM NaCl), TSE III (0.25 M LiCl, 1% NP-40, 1% deoxycholate, 1 mM EDTA, 10 mM Tris-HCl at pH 8.1), and TSE IV (10 mM Tris-HCl at pH 8.1, 150 mM NaCl, 1 mM EDTA). Cross-linking was reversed overnight at 65°C in TSE V (20 mM Tris-HCl at pH 7.5, 150 mM NaCl, 2 mM EDTA, 1% SDS). DNA fragments were purified with a QIAquick spin kit (Qiagen) and eluted in 30 µL of elution buffer. qPCR was performed with SYBR Green (Fermentas) using a CFX384 real-time PCR device (Bio-Rad). BMAL1 binding within the promoter region of the human *REVERBα* gene; qPCR was performed with the primers 5′-CCTTCTCTGGACTTTGCCCT-3′ (forward) and 5′-AAACCTTGCAAACGTGAGGG-3′ (reverse).

Fluorescence recovery after photobleaching (FRAP)

To measure the mobility of YFP-BMAL1 at the *Dbp* gene array in NIH3T3 cells (Stratmann et al. 2012) in presence or absence of endogenous PPP4R2 (see RNAi-mediated knockdown), confocal microscopy of live cells was performed using a Nikon Spinning Disk Confocal CSU-X (Nikon Instruments Europe BV) with a 60× (1.27 numerical aperture) water immersion objective in a climate chamber at 37°C under 5% CO_2. Cells were seeded on glass-bottom #1.5H µ-slides (IBIDI), and image acquisition was performed in Flurobrite medium (Thermo) supplemented with 2% FBS, 1:100 PenStrep, and 1× GlutaMax at 37°C and 5% CO_2. The spot-like nuclear fluorescence signals were bleached (488 nm, 100% intensity), and recovery of fluorescence was observed over 200 sec by acquiring images (emission filter 525 nm, 50-nm bandwidth) every 0.5 sec for the first 25 sec and every 10 sec for the remainder of the imaging period. For analysis, both the bleached spots and control regions were measured in the respective nuclei. Intensity values were extracted, and bleaching due to imaging was corrected using the control regions of the respective nuclei. The initial fluorescence of the spots was set to 1.0.

Activity monitoring of flies and behavioral analysis

Flies were raised in a 12-h:12-h light/dark (LD) cycle on standard *Drosophila* medium (0.7% agar, 1.0% soy flour, 8.0% polenta/maize, 1.8% yeast, 8.0% malt extract, 4.0% molasses, 0.8% propionic acid, 2.3% nipagen) at 25° C and 60% relative humidity. *tim-gal4:27* and *tim-gal4:62* drive Gal4 expression in all clock cells (Kaneko and Hall 2000), while *Pdf-Gal4* activity is restricted to the ~16 clock neurons expressing the neuropeptide pigment dispersing factor (PDF) (Renn et al. 1999). To reduce *PPP2R2r* expression, these Gal4 driver lines where crossed to two independent *UAS-PPP2R2r* RNAi lines (RNAi-1: *TRiP BL26296* and RNAi-2: *v105399*) obtained from the Bloomington and VDRC stock centers, respectively. To enhance the RNAi-mediated knockdown, the *tim-gal4:27* lines were combined with *UAS-dicer* (Dietzl et al. 2007). To overexpress *PPP2R2r*, the same Gal4

lines were crossed to the *EP307* line (Rorth 1996) carrying an *UAS* insertion immediately upstream of the *PPP2R2r* transcription start site (Bloomington Stock Center BL10106). Analysis of locomotor activity of 4- to 5-d-old male flies was performed using the *Drosophila* activity monitor system (DAM2; Trikinetics, Inc.) with individual flies in recording tubes containing food (2% agar, 4% sucrose). DAM2 activity monitors containing flies were located inside a light- and temperature-controlled incubator (Percival Scientific, Inc.), where fly activity was monitored for 4 d in rectangular 12-h:12-h LD (~1000 lux generated by 17-W F17T8/TL841 cool white Hg compact fluorescent lamps; Philips) followed by 7 d in constant darkness and temperature (25°C). Plotting of behavioral activity and period calculations were performed using a signal processing toolbox (Levine et al. 2002) implemented in MATLAB (MathWorks) as described (Chen et al. 2018). Period length values and their significance (*RS* values) were determined using the autocorrelation function, and period values with an $RS \geq 1.5$ were classified as rhythmic (Levine et al. 2002). For the statistical analysis of the data, estimation statistics were used. This approach gives a more informative way to analyze and interpret results (Ho et al. 2019). It focuses on the effect size, as opposed to significance testing. While significance testing (*P*-values) focuses on the acceptance or rejection of the null hypothesis, estimation stats focus on the magnitude of the effect size (i.e., mean difference) and its precision (Ho et al. 2019). Data were analyzed using DABEST (Ho et al. 2019), using the website https://www.estimationstats.com/#; as described (Versteven et al. 2020).

Competing interest statement

The authors declare no competing interests.

Acknowledgments

We thank A. Grudziecki and B. Koller for excellent technical support, M. Brunner (Ruprecht-Karls-University, Heidelberg, Germany) and U. Schibler (University of Geneva, Switzerland) for materials. We thank the Advanced Medical Bioimaging Core Facility (AMBIO) of the Charité for support in acquisition of the imaging data. This work was funded by the Deutsche Forschungsgemeinschaft (DFG [German Research Foundation]: SFB740 and TRR186; project no. 278001972).

Author contributions: S. Klemz, T.W., S. Korge, M.R., R.K., N.C.F., I.K., A.K.F., and E.D.H. performed experiments. S. Klemz, T.W., S. Korge, R.K., B.M., E.D.H., R.S., and A.K. designed experiments and analyzed data. R.S. and A.K. wrote the paper. A.K. oversaw the project.

References

Agrawal P, Hardin PE. 2016. An RNAi screen to identify protein phosphatases that function within the *Drosophila* circadian clock. *G3* **6:** 4227–4238. doi:10.1534/g3.116.035345

Aryal RP, Kwak PB, Tamayo AG, Gebert M, Chiu P-L, Walz T, Weitz CJ. 2017. Macromolecular assemblies of the mammalian circadian clock. *Mol Cell* **67:** 770–782.e6. doi:10.1016/j.molcel.2017.07.017

Brand AH, Perrimon N. 1993. Targeted gene expression as a means of altering cell fates and generating dominant phenotypes. *Development* **118:** 401–415. doi:10.1242/dev.118.2.401

Brautigan DL, Shenolikar S. 2018. Protein serine/threonine phosphatases: keys to unlocking regulators and substrates. *Annu Rev Biochem* **87:** 921–964. doi:10.1146/annurev-biochem-062917-012332

Cao X, Yang Y, Selby CP, Liu Z, Sancar A. 2021. Molecular mechanism of the repressive phase of the mammalian circadian clock. *Proc Natl Acad Sci* **118:** e2021174118. doi:10.1073/pnas.2021174118

Chen C, Xu M, Anantaprakorn Y, Rosing M, Stanewsky R. 2018. *nocte* is required for integrating light and temperature inputs in circadian clock neurons of *Drosophila*. *Curr Biol* **28:** 1595–1605.e3. doi:10.1016/j.cub.2018.04.001

Cohen PTW, Philp A, Vázquez-Martin C. 2005. Protein phosphatase 4 - from obscurity to vital functions. *FEBS Lett* **579:** 3278–3286.

Dietzl G, Chen D, Schnorrer F, Su K-C, Barinova Y, Fellner M, Gasser B, Kinsey K, Oppel S, Scheiblauer S, et al. 2007. A genome-wide transgenic RNAi library for conditional gene inactivation in *Drosophila*. *Nature* **448:** 151–156. doi:10.1038/nature05954

Edery I, Zwiebel LJ, Dembinska ME, Rosbash M. 1994. Temporal phosphorylation of the *Drosophila* period protein. *Proc Natl Acad Sci* **91:** 2260–2264. doi:10.1073/pnas.91.6.2260

Finger A-M, Kramer A. 2021. Peripheral clocks tick independently of their master. *Genes Dev* **35:** 304–306. doi:10.1101/gad.348305.121

Finger A, Dibner C, Kramer A. 2020. Coupled network of the circadian clocks: a driving force of rhythmic physiology. *FEBS Lett* **594:** 2734–2769. doi:10.1002/1873-3468.13898

Gallego M, Kang H, Virshup DM. 2006. Protein phosphatase 1 regulates the stability of the circadian protein PER2. *Biochem J* **399:** 169–175. doi:10.1042/BJ20060678

Gekakis N. 1998. Role of the CLOCK protein in the mammalian circadian mechanism. *Science* **280:** 1564–1569.

Grosbellet E, Dumont S, Schuster-Klein C, Guardiola-Lemaitre B, Pevet P, Criscuolo F, Challet E. 2016. Circadian phenotyping of obese and diabetic db/db mice. *Biochimie* **124:** 198–206. doi:10.1016/j.biochi.2015.06.029

He Q, Liu Y. 2005. Molecular mechanism of light responses in *Neurospora*: from light-induced transcription to photoadaptation. *Genes Dev* **19:** 2888–2899. doi:10.1101/gad.1369605

He Q, Cha J, He Q, Lee HC, Yang Y, Liu Y. 2006. CKI and CKII mediate the FREQUENCY-dependent phosphorylation of the WHITE COLLAR complex to close the *Neurospora* circadian negative feedback loop. *Genes Dev* **20:** 2552–2565. doi:10.1101/gad.1463506

Hirano A, Fu Y-H, Ptáček LJ. 2016. The intricate dance of post-translational modifications in the rhythm of life. *Nat Struct Mol Biol* **23:** 1053–1060. doi:10.1038/nsmb.3326

Ho J, Tumkaya T, Aryal S, Choi H, Claridge-Chang A. 2019. Moving beyond *P* values: data analysis with estimation graphics. *Nat Methods* **16:** 565–566. doi:10.1038/s41592-019-0470-3

Kaneko M, Hall JC. 2000. Neuroanatomy of cells expressing clock genes in *Drosophila*: transgenic manipulation of the period and timeless genes to mark the perikarya of circadian pacemaker neurons and their projections. *J Comp Neurol* **422:** 66–94. doi:10.1002/(SICI)1096-9861(20000619)422:1<66::AID-CNE5>3.0.CO;2-2

King DP, Zhao Y, Sangoram AM, Wilsbacher LD, Tanaka M, Antoch MP, Steeves TDL, Vitaterna MH, Kornhauser JM, Lowrey PL, et al. 1997. Positional cloning of the mouse circadian clock gene. *Cell* **89:** 641–653. doi:10.1016/S0092-8674(00)80245-7

Koike N, Yoo S-H, Huang H-C, Kumar V, Lee C, Kim T-K, Takahashi JS. 2012. Transcriptional architecture and chromatin

landscape of the core circadian clock in mammals. *Science* **338:** 349–354. doi:10.1126/science.1226339

Kondratov RV. 2003. BMAL1-dependent circadian oscillation of nuclear CLOCK: posttranslational events induced by dimerization of transcriptional activators of the mammalian clock system. *Genes Dev* **17:** 1921–1932. doi:10.1101/gad.1099503

Kramer A. 2015. When the circadian clock becomes blind. *Science* **347:** 476–477. doi:10.1126/science.aaa5085

Kwon I, Lee J, Chang SH, Jung NC, Lee BJ, Son GH, Kim K, Lee KH. 2006. BMAL1 shuttling controls transactivation and degradation of the CLOCK/BMAL1 heterodimer. *Mol Cell Biol* **26:** 7318–7330. doi:10.1128/MCB.00337-06

Larrondo LF, Olivares-Yanez C, Baker CL, Loros JJ, Dunlap JC. 2015. Decoupling circadian clock protein turnover from circadian period determination. *Science* **347:** 1257277–1257277. doi:10.1126/science.1257277

Lee C, Etchegaray J-P, Cagampang FRA, Loudon ASI, Reppert SM. 2001. Posttranslational mechanisms regulate the mammalian circadian clock. *Cell* **107:** 855–867. doi:10.1016/S0092-8674(01)00610-9

Lee HM, Chen R, Kim H, Etchegaray J-P, Weaver DR, Lee C. 2011. The period of the circadian oscillator is primarily determined by the balance between casein kinase 1 and protein phosphatase 1. *Proc Natl Acad Sci* **108:** 16451–16456. doi:10.1073/pnas.1107178108

Levine JD, Funes P, Dowse HB, Hall JC. 2002. Advanced analysis of a cryptochrome mutation's effects on the robustness and phase of molecular cycles in isolated peripheral tissues of *Drosophila*. *BMC Neurosci* **3:** 5. doi:10.1186/1471-2202-3-5

Maier B, Wendt S, Vanselow JT, Wallach T, Reischl S, Oehmke S, Schlosser A, Kramer A. 2009. A large-scale functional RNAi screen reveals a role for CK2 in the mammalian circadian clock. *Genes Dev* **23:** 708–718. doi:10.1101/gad.512209

Maier B, Lorenzen S, Finger A-M, Herzel H, Kramer A. 2021. Searching novel clock genes using RNAi-based screening. *Methods Mol Biol* **2130:** 103–114. doi:10.1007/978-1-0716-0381-9_8

Narasimamurthy R, Virshup DM. 2021. The phosphorylation switch that regulates ticking of the circadian clock. *Mol Cell* **81:** 1133–1146. doi:10.1016/j.molcel.2021.01.006

Partch CL, Shields KF, Thompson CL, Selby CP, Sancar A. 2006. Posttranslational regulation of the mammalian circadian clock by cryptochrome and protein phosphatase 5. *Proc Natl Acad Sci* **103:** 10467–10472. doi:10.1073/pnas.0604138103

Reischl S, Kramer A. 2011. Kinases and phosphatases in the mammalian circadian clock. *FEBS Lett* **585:** 1393–1399. doi:10.1016/j.febslet.2011.02.038

Renn SCP, Park JH, Rosbash M, Hall JC, Taghert PH. 1999. A pdf neuropeptide gene mutation and ablation of PDF neurons each cause severe abnormalities of behavioral circadian rhythms in *Drosophila*. *Cell* **99:** 791–802. doi:10.1016/S0092-8674(00)81676-1

Ripperger JA, Schibler U. 2006. Rhythmic CLOCK-BMAL1 binding to multiple E-box motifs drives circadian Dbp transcription and chromatin transitions. *Nat Genet* **38:** 369–374. doi:10.1038/ng1738

Robles MS, Humphrey SJ, Mann M. 2017. Phosphorylation is a central mechanism for circadian control of metabolism and physiology. *Cell Metab* **25:** 118–127. doi:10.1016/j.cmet.2016.10.004

Rorth P. 1996. A modular misexpression screen in *Drosophila* detecting tissue-specific phenotypes. *Proc Natl Acad Sci* **93:** 12418–12422. doi:10.1073/pnas.93.22.12418

Sahar S, Zocchi L, Kinoshita C, Borrelli E, Sassone-Corsi P. 2010. Regulation of BMAL1 protein stability and circadian function by GSK3β-mediated phosphorylation. *PLoS One* **5:** e8561. doi:10.1371/journal.pone.0008561

Schafmeier T, Haase A, Káldi K, Scholz J, Fuchs M, Brunner M. 2005. Transcriptional feedback of *Neurospora* circadian clock gene by phosphorylation-dependent inactivation of its transcription factor. *Cell* **122:** 235–246. doi:10.1016/j.cell.2005.05.032

Schmutz I, Wendt S, Schnell A, Kramer A, Mansuy IM, Albrecht U. 2011. Protein phosphatase 1 (PP1) is a post-translational regulator of the mammalian circadian clock. *PLoS One* **6:** e21325. doi:10.1371/journal.pone.0021325

Stratmann M, Suter DM, Molina N, Naef F, Schibler U. 2012. Circadian Dbp transcription relies on highly dynamic BMAL1-CLOCK interaction with E boxes and requires the proteasome. *Mol Cell* **48:** 277–287. doi:10.1016/j.molcel.2012.08.012

Tamaru T, Hirayama J, Isojima Y, Nagai K, Norioka S, Takamatsu K, Sassone-Corsi P. 2009. CK2α phosphorylates BMAL1 to regulate the mammalian clock. *Nat Struct Mol Biol* **16:** 446–448. doi:10.1038/nsmb.1578

Tansey WP. 2001. Transcriptional activation: risky business. *Genes Dev* **15:** 1045–1050. doi:10.1101/gad.896501

Thomas D, Tyers M. 2000. Transcriptional regulation: kamikaze activators. *Curr Biol* **10:** R341–R343. doi:10.1016/S0960-9822(00)00462-0

Vanselow K, Kramer A. 2007. Role of phosphorylation in the mammalian circadian clock. *Cold Spring Harb Symp Quant Biol* **72:** 167–176. doi:10.1101/sqb.2007.72.036

Vanselow K, Vanselow JT, Westermark PO, Reischl S, Maier B, Korte T, Herrmann A, Herzel H, Schlosser A, Kramer A. 2006. Differential effects of PER2 phosphorylation: molecular basis for the human familial advanced sleep phase syndrome (FASPS). *Genes Dev* **20:** 2660–2672. doi:10.1101/gad.397006

Versteven M, Ernst K-M, Stanewsky R. 2020. A robust and self-sustained peripheral circadian oscillator reveals differences in temperature compensation properties with central brain clocks. *iScience* **23:** 101388. doi:10.1016/j.isci.2020.101388

Wang J, Mauvoisin D, Martin E, Atger F, Galindo AN, Dayon L, Sizzano F, Palini A, Kussmann M, Waridel P, et al. 2017. Nuclear proteomics uncovers diurnal regulatory landscapes in mouse liver. *Cell Metab* **25:** 102–117. doi:10.1016/j.cmet.2016.10.003

Wang B, Kettenbach AN, Zhou X, Loros JJ, Dunlap JC. 2019. The phospho-code determining circadian feedback loop closure and output in Neurospora. *Mol Cell* **74:** 771–784.e3. doi:10.1016/j.molcel.2019.03.003

Yoo S-H, Yamazaki S, Lowrey PL, Shimomura K, Ko CH, Buhr ED, Siepka SM, Hong H-K, Oh WJ, Yoo OJ, et al. 2004. PERIOD2::LUCIFERASE real-time reporting of circadian dynamics reveals persistent circadian oscillations in mouse peripheral tissues. *Proc Natl Acad Sci* **101:** 5339–5346. doi:10.1073/pnas.0308709101

Yoshitane H, Fukada Y. 2021. Circadian phosphorylation of CLOCK and BMAL1. *Methods Mol Biol* **2130:** 195–203. doi:10.1007/978-1-0716-0381-9_15

Yoshitane H, Takao T, Satomi Y, Du N-H, Okano T, Fukada Y. 2009. Roles of CLOCK phosphorylation in suppression of

E-box-dependent transcription. *Mol Cell Biol* **29:** 3675–3686. doi:10.1128/MCB.01864-08

Zhao W-N, Malinin N, Yang F-C, Staknis D, Gekakis N, Maier B, Reischl S, Kramer A, Weitz CJ. 2007. CIPC is a mammalian circadian clock protein without invertebrate homologues. *Nat Cell Biol* **9:** 268–275. doi:10.1038/ncb1539

Zhao H, Huang X, Jiao J, Zhang H, Liu J, Qin W, Meng X, Shen T, Lin Y, Chu J. 2015. Protein phosphatase 4 (PP4) functions as a critical regulator in tumor necrosis factor (TNF)-α-induced hepatic insulin resistance. *Sci Rep* **5:** 18093. doi:10.1038/srep18093

Zhou G, Mihindukulasuriya KA, MacCorkle-Chosnek RA, Van Hooser A, Hu MC-T, Brinkley BR, Tan T-H. 2002. Protein phosphatase 4 is involved in tumor necrosis factor-α-induced activation of c-Jun N-terminal kinase. *J Biol Chem* **277:** 6391–6398. doi:10.1074/jbc.M107014200